no detectable cross-reactivity for H-2^b (*10*).
12. The origin of the small number of CD44^{hi} 1B2$^+$ cells in 2C mice is unknown. These cells may be recent thymic emigrants because about 5% of thymic emigrants in normal mice are CD44^{hi} (*4*).
13. The possibility that poly(I:C)-induced proliferation of T cells adoptively transferred to β_2M^- mice reflected TCR contact with residual class I molecules is unlikely for two reasons. First, the injected β_2M^- CD8$^+$ cells were thoroughly depleted of non–T cells. Second, the low concentration of cell-surface class I molecules in β_2M^- mice causes only minimal positive selection of CD8$^+$ cells in the thymus and is essentially nonimmunogenic for normal CD8$^+$ cells.
14. M. Roederer, *Nature Med.* **1**, 621 (1995).
15. C. Tanchot and B. Rocha, *Eur. J. Immunol.* **25**, 2127 (1995).
16. E. B. Bell, S. M. Sparshott, M. T. Drayson, W. L. Ford, *J. Immunol.* **139**, 1379 (1987).
17. Although T cell proliferation in nude rodent hosts can occur under specific pathogen-free conditions, the possibility that these hosts harbor undetected viral infections cannot be discounted.
18. H. von Boehmer and K. Hafen, *J. Exp. Med.* **177**, 891 (1993).
19. B. Rocha, N. Dautigny, P. Pereira, *Eur. J. Immunol.* **19**, 905 (1989).
20. S. Oehen, H. Waldner, T. M. Kündig, H. Hengartner, R. Zinkernagel, *J. Exp. Med.* **176**, 1273 (1992).
21. D. Gray and P. Matzinger, *ibid.* **174**, 969 (1991).
22. A. Mullbacher, *ibid.* **179**, 317 (1994); S. Hou, L. Hyland, K. W. Ryan, A. Portner, P. C. Doherty, *Nature* **369**, 652 (1994).
23. L. Bruno, J. Kirberg, H. von Boehmer, *Immunity* **2**, 37 (1995).
24. P. C. L. Beverley, *Immunol. Today* **11**, 203 (1990).
25. R. A. Tripp, S. Hou, P. C. Doherty, *J. Immunol.* **154**, 5870 (1995).
26. D. Kyburz *et al, Eur. J. Immunol.* **23**, 1956 (1993).
27. F. J. Dutko and M. B. A. Oldstone, *J. Gen. Virol.* **64**, 1689 (1983).
28. J. L. Whitton, P. J. Southern, M. B. A. Oldstone, *Virology* **162**, 321 (1988).
29. E. K. Gao, D. Lo, J. Sprent, *J. Exp. Med.* **171**, 1101 (1990).
30. M. Zijlstra, E. Li, F. Sajjadi, S. Subramani, R. Jaenisch, *Nature* **342**, 435 (1989).
31. J. Sprent and M. Schaefer, *J. Exp. Med.* **162**, 2068 (1985).
32. D. M. Kranz, S. Tonegawa, H. N. Eisen, *Proc. Natl. Acad. Sci. U.S.A.* **81**, 7922 (1984).
33. I. Gresser, M. G. Tovey, M.-T. Bandu, M. Chantal, D. Brouty-Boye, *J. Exp. Med.* **144**, 1305 (1976).
34. B6 mice were thymectomized at 5 to 6 weeks of age and left for 4 weeks before viral infection. Viruses used were the Armstrong 53b strain of LCMV (*27*); the Mudd-Summers strain of the Indiana serotype of VSV; and a thymidine kinase–negative VV recombinant, VVSC11, which expresses β-galactosidase (*28*). Viral titers were determined by plaque assay on Vero (LCMV and VSV) or 143TK$^-$ (VV) cells (*27*). All virus stocks were free of mycoplasma contamination. Mice were intravenously (iv) injected with LCMV [2×10^6 plaque-forming units (PFU)] or VSV (5×10^5 PFU), or were intraperitoneally (ip) injected with VV (2×10^6 PFU), and then immediately given BrdU (Sigma) drinking water (0.8 mg/ml) (*4*). BrdU water was made fresh and changed daily. LN cells were stained for flow cytometry with mAbs to CD8-PE (Gibco-BRL, Gaithersburg, MD), to CD4-PE (Collaborative Biomedical Products, Bedford, MA), to CD44-biotin (IM7.8.1), or to Ly-6C–biotin (Pharmingen, San Diego, CA); with streptavidin-RED613 (Gibco-BRL); and, after fixation, with mAb to BrdU-FITC (Becton Dickinson, Mountainview, CA) (*4*). Stained cells were analyzed on a FACScan flow cytometer (Becton Dickinson).
35. For poly(I:C) experiments, mice were injected ip with poly(I:C) (150 μg) (Sigma) in 150 μl of phosphate-buffered saline (PBS). For 4-hour BrdU labeling, mice were injected ip with 1 mg of BrdU in 200 μl of PBS and then given BrdU drinking water for 4 hours before being killed. Bone marrow chimeras were constructed by injection of T-depleted bone marrow into B6 mice irradiated with 10Gy (*29*). Donors were either β_2M^- (*30*) or B6 2C (*10*) mice. Six weeks after construction of ($\beta_2M^- \rightarrow$ B6) chimeras, purified CD8$^+$ LN cells were prepared by depletion of CD4$^+$, MHC class I$^+$ and class II$^+$ cells with antibody plus complement, followed by positive panning on plates coated with antibody to CD8 (*31*). Class I$^-$ CD8$^+$ cells (8×10^5) were injected iv into β_2M^- recipients. Six days later, these mice were injected ip with poly(I:C) or PBS. Three-color staining of cells for flow cytometric analysis was carried out as in Fig. 1, with the use of additional mAbs to CD25-biotin (7D4) and CD69-biotin (Pharmingen). For analysis of CD8$^+$ 1B2$^+$ CD44^{lo} and CD44^{hi} cells in ATx 2C mice, cells were stained with mAb to CD8-CyChrome (Pharmingen), 1B2-biotin (*32*), Texas Red–streptavidin (Gibco-BRL), and mAb to CD44-PE (Pharmingen) before being stained with mAb to BrdU-FITC. Four-color analysis was done with a FACStar Plus flow cytometer (Becton Dickinson).
36. To test the ability of anti–IFN I to inhibit poly(I:C)-induced proliferation, ATx B6 mice were injected iv three times with either adsorbed neutralizing antiserum to murine IFN α/β (neutralizing titer: 5.3×10^{-5} against 8 IU of murine IFN α/β) (*33*) or normal adsorbed sheep serum. Mice were injected with 0.2 ml of sera 2 hours before and 24 and 48 hours after being injected ip with either 50 μg of poly(I:C) in 200 μl of PBS or with 200 μl of PBS alone. BrdU water was given to the mice from the time of PBS or poly(I:C) injection. To test the effect of murine IFN I in vivo, ATx B6 mice received a single iv injection of either 4.4×10^5 U of purified murine IFN-β (Lee Biomolecular Laboratory, San Diego, CA) or an equivalent volume (0.45 ml) of mock IFN α/β (Lee Biomolecular Laboratory) and were immediately started on BrdU drinking water. Staining of LN and spleen cells for flow cytometry was carried out as described in Fig. 1.
37. For adoptive transfer experiments (shown in Fig. 4C), B6 2C LN cells (5.5×10^6) were injected iv plus or minus T-depleted (*31*) B10.D2 (H-2^d) spleen cells (2.6×10^7) into normal B6 mice. BrdU water was given for 7 days from the time of immunization; where indicated, mice were injected ip with a single dose of 100 μg of poly(I:C) 1 or 2 days later; the effects of poly(I:C) given 1 or 2 days after immunization were quite similar, and pooled data for these time points are shown. Mice were either killed 7 days after injection of cells or transferred to normal water for a further 4 weeks. The number of BrdU$^+$ 1B2$^+$ CD8$^+$ cells was calculated from total cell counts of pooled LNs and spleens. Experiments 1 and 2 represent independent experiments.
38. We thank M. B. A. Oldstone for advice on viral experiments, D. Y. Loh for 2C mice, I. Gresser for providing antiserum to IFN, T. Knapp for assistance with four-color analysis, and B. Marchand for typing the manuscript. Supported by grants CA38355, CA25803, AI21487, and AI32068 from the USPHS and by a Centennial Fellowship from the Medical Research Council of Canada (to D.F.T.). This is publication 9662-IMM from the Scripps Research Institute.

24 January 1996; accepted 26 April 1996

Nonselective and $G_{\beta\gamma}$-Insensitive *weaver* K^+ Channels

Betsy Navarro, Matthew E. Kennedy, Bratislav Velimirović, Deepti Bhat, Andrew S. Peterson, David E. Clapham*

Homozygous *weaver* mice are profoundly ataxic because of the loss of granule cell neurons during cerebellar development. This granule cell loss appears to be caused by a genetic defect in the pore region (Gly$^{156} \rightarrow$ Ser) of the heterotrimeric guanine nucleotide–binding protein (G protein)–gated inwardly rectifying potassium (K^+) channel subunit (GIRK2). A related subunit, GIRK1, associates with GIRK2 to constitute a neuronal G protein–gated inward rectifier K^+ channel. The *weaver* allele of the GIRK2 subunit (*wv*GIRK2) caused loss of K^+ selectivity when expressed either as *wv*GIRK2 homomultimers or as GIRK1-*wv*GIRK2 heteromultimers. The mutation also led to loss of sensitivity to G protein βγ dimers. Expression of *wv*GIRK2 subunits led to increased cell death, presumably as a result of basal nonselective channel opening.

A point mutation in the pore region of the GIRK2 K^+ channel subunit appears to cause cerebellar granule cell loss in *weaver* mice (*1*). G protein–gated inward rectifier K^+ channels are heteromultimers of GIRK1 and CIR [cardiac inward rectifier or GIRK4 (*2*, *3*)] or GIRK1 and GIRK2 subunits (*4*, *5*) that are directly bound and gated by $G_{\beta\gamma}$ subunits (*6*). When expressed alone, GIRK2 or CIR subunits display unusual kinetics [fast with variable amplitude (*3*, *5*)] that presumably represent homomultimeric channels. GIRK1 does not appear to form detectable homomultimeric K^+ channels in transfected Chinese hamster ovary (CHO) cells or human embryonic kidney (HEK; A293) cells (*2*) and forms a K^+ channel in *Xenopus* oocytes only by interacting with an intrinsic *Xenopus* CIR homolog, XIR (*7*). Coexpression of GIRK1 and GIRK2 subunits results in channels with conductance, kinetics, and regulation similar to those of GIRK1-CIR channels, which form the acetylcholine (ACh)–gated inward rectifier K^+ channel (I_{KACh}) in native heart tissue (*2*, *3*).

GIRK1 and GIRK2 mRNA are colocalized in the early postnatal mouse cerebellum, when *weaver* mice granule cells are lost (*8*). In situ hybridizations identified GIRK1 ex-

B. Navarro, M. E. Kennedy, B. Velimirović, D. E. Clapham, Department of Pharmacology, Mayo Foundation, Rochester, MN 55905, USA.
D. Bhat and A. S. Peterson, Departments of Genetics and Neurobiology, Duke University Medical Center, Durham, NC 27710, USA.
*To whom correspondence should be addressed.

pression throughout the cerebellar external granule cell layer, Purkinje neurons, and postmigratory granule cells (Fig. 1A) (9). Like GIRK1, GIRK2 is expressed throughout the external granule cell layer, but this expression is increased in the developing internal granule cell layer.

GIRK1 and GIRK2 coexpression (GIRK1-GIRK2) yielded characteristic $G_{\beta\gamma}$-activated K^+ channels (*4*, *5*). Physical association of GIRK1 and GIRK2 was evidenced by coimmunoprecipitation of epitope-tagged K^+ channel subunits in [^{35}S]methionine-labeled COS-M7 cells (Fig. 1B) (*10*). When GIRK1, GIRK2, or *wv*GIRK2 was expressed alone, immunoprecipitates of epitope-tagged channel subunits displayed the expected 55-, 48-, and 48-kD unglycosylated bands, respectively, which were not present in immunoprecipitates from control COS-M7 cells. GIRK2 or *wv*GIRK2 subunits coimmunoprecipitated GIRK1 when coexpressed (Fig. 1B, lanes 4 and 5). These data suggest that the inward rectifier in the cerebellum is composed of GIRK1 and GIRK2 subunits.

Whole-cell currents in CHO cells coexpressing GIRK1-GIRK2 were several times larger than GIRK1-*wv*GIRK2 currents. Unexpectedly, homomultimeric *wv*GIRK2 currents were as large as GIRK1-*wv*GIRK2 currents and were larger than homomultimeric GIRK2 currents (Fig. 1C) (*11*). Single-channel analysis of *wv*GIRK2 or GIRK1-*wv*GIRK2 channels revealed characteristic short-lived openings similar to those described for GIRK2 homomultimers (*5*). Since GIRK1 homomultimers do not form functional channels (*2*–*5*), we conclude that *wv*GIRK2-containing channels are defective.

Because the first glycine of the K^+ channel pore signature sequence Gly-Tyr-Gly (*1*) is mutated to serine in the *wv*GIRK2 subunit ($Gly^{156} \rightarrow Ser$), we examined the selectivity of *wv*GIRK2-containing channel complexes. The reversal potentials of currents in CHO cells expressing GIRK1-GIRK2, GIRK1-*wv*GIRK2 heteromultimers, or *wv*GIRK2 homomultimers were measured under bi-ionic conditions (Fig. 2, A to C). Calculated permeability ratios (P_X/P_K) for GIRK1-GIRK2 channels indicated high K^+ selectivity ($P_{Na}/P_K = 0.03 \pm 0.004$) and Cs^+ blockade (no measurable conductance in 138 mM external Cs^+) (Fig. 2A). GIRK1-*wv*GIRK2 channels had permeability ratios of 0.93 ± 0.02 for P_{Cs}/P_K and 0.74 ± 0.02 for P_{Na}/P_K. For *wv*GIRK2 homomultimers, the ratios were 0.99 ± 0.05 for P_{Cs}/P_K and 0.94 ± 0.04 for P_{Na}/P_K (Fig. 2D). We did not detect Ca^{2+} permeability in up to 80 mM external Ca^{2+}. The *wv*GIRK2-containing channels were not permeant to anions; neither replacement of extracellular KCl with *K*-methanesulfonate nor substitution of 110 mM internal Cl^- by equimolar aspartic acid altered the inward current. We conclude from the permeability measurements that *wv*GIRK2 produced a nonselective cationic channel. Moreover, the greater Na^+ macroscopic conductance and permeability ratio of presumed homomultimeric *wv*GIRK2 relative to those of GIRK1-*wv*GIRK2 channels suggest that both *wv*GIRK2 and GIRK1 contribute to the pore. Previous site-directed mutagenesis at the corresponding residue of the outward delayed rectifier *shaker* K^+ channel also caused a loss of selectivity (*12*).

GIRK1-GIRK2 single channels measured in inside-out patches from CHO cells were strongly activated [as indicated by a 120-fold increase in Np_o, where Np_o = integrated current/($i \cdot 6$ s) and i is single-channel current] by the addition of 20 nM purified $G_{\beta\gamma}$ or 10 μM guanosine 5′-*O*-(3-thiotriphosphate) (GTP-γ-S) to the bath (Fig. 3, A and B) (*5*, *6*). In contrast, 20 to 60 nM $G_{\beta\gamma}$ did not enhance the activity of GIRK1-*wv*GIRK2 or homomultimeric *wv*GIRK2 channels. There was a small but reproducible increase in channel activity (a sevenfold increase in Np_o) when 1 to 10 μM GTP-γ-S was added to the bath in the presence of 100 μM adenosine triphosphate (ATP) (Fig. 3A, bottom trace); this increase was similar to that observed for homomultimeric GIRK2 or CIR (*2*, *3*, *5*, *13*). These data demonstrate that channels that contain *wv*GIRK2 subunits not only lose their selectivity but also are no longer tightly linked to the G protein pathway.

ACh increased net inwardly rectifying K^+ current up to 10 μA in oocytes expressing GIRK1-GIRK2 and muscarinic receptor type 2 (m2). Bypassing the receptor by expressing $G_{\beta 1\gamma 2}$ with GIRK2 yielded 10 to 16 μA of ACh-independent current (*5*). When *wv*GIRK2 was substituted for GIRK2 in coinjections with GIRK1, peak current

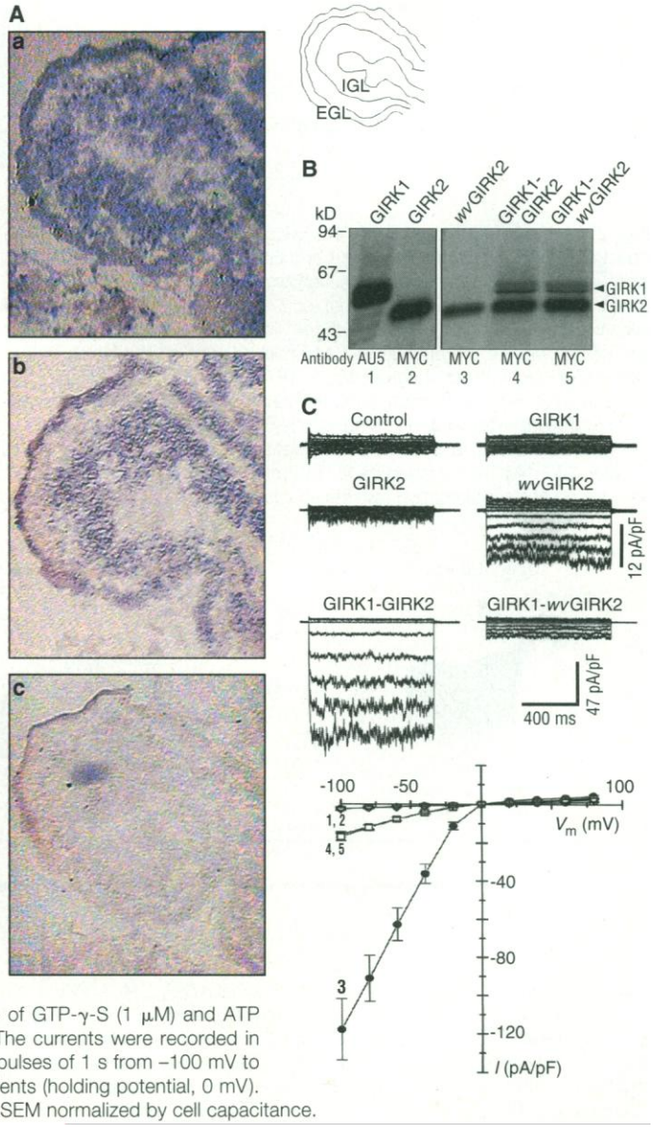

Fig. 1. (**A**) GIRK1 and GIRK2 are expressed in the cerebellar external granule cell layer. Adjacent sagittal sections from a 6-day-old mouse brain were hybridized with an antisense probe for GIRK1 (a), an antisense probe for GIRK2 (b), or a sense probe for GIRK2 (c). EGL, external granule cell layer; IGL, internal granule cell layer. GIRK1 and GIRK2 sense controls were similar. (**B**) Coexpressed GIRK1-GIRK2 or GIRK1-*wv*GIRK2 form heteromultimers. COOH-terminal MYC- tagged GIRK2 or *wv*GIRK2 coimmunoprecipitate COOH-terminal AU5-tagged GIRK1 when coexpressed in COS-M7 cells. (**C**) Repression of functional expression of heteromultimeric K^+ channels in a cell expressing *wv*GIRK2. Whole-cell current traces and current-voltage relations from CHO cells transiently transfected with pCDNA1/amp (control) or GIRK1 (n = 25) (▽, **1**), GIRK2 (n = 7) (○, **2**), GIRK1-GIRK2 (n = 12) (●, **3**), *wv*GIRK2 (n = 14) (□, **4**), and GIRK1-*wv*GIRK2 (n = 14) (■, **5**). Whole-cell currents were recorded in the presence of GTP-γ-S (1 μM) and ATP (100 μM) in the pipette. The currents were recorded in response to depolarizing pulses of 1 s from −100 mV to +80 mV in 20-mV increments (holding potential, 0 mV). Points represent mean ± SEM normalized by cell capacitance.

was reduced (0.5 ± 0.2 μA at −100 mV in 96 mM external K^+) and was insensitive to ACh. In addition, E_{rev} (the reversal potential) shifted only 14 mV per 10-fold change in external K^+, which indicated a loss of K^+ selectivity. Oocytes injected with *wv*GIRK2 alone, *wv*GIRK2 plus $G_{\beta 1\gamma 2}$, or *wv*GIRK2 plus m2 displayed small currents similar to those for oocytes injected with GIRK1-*wv*GIRK2 plus m2. Interestingly, *wv*GIRK2 had a dominant negative effect in GIRK1-GIRK2-*wv*GIRK2 and GIRK1-CIR-*wv*GIRK2 coexpressions.

The expression of *wv*GIRK2 led to markedly reduced oocyte and CHO cell survival. Most of the oocytes expressing *wv*GIRK2 were obviously lysed after several days. The fraction of oocytes surviving at 60 hours after injection was 31/42 (74%) for GIRK1-GIRK2, 7/41 (17%) for GIRK1-*wv*GIRK2, 2/40 (5%) for *wv*GIRK2, and 0/15 for GIRK1-CIR-*wv*GIRK2. The survival of CHO cells was also reduced by expression of *wv*GIRK2, as measured by the percentage of MYC-tagged *wv*GIRK2 intact cells with respect to all labeled cells and cell remnants. Survival per cover slip was 113/126 (90%) for GIRK2 alone, 190/242 (79%) for GIRK1-GIRK2, 120/245 (49%) for GIRK1-*wv*GIRK2, and 13/59 (22%) for *wv*GIRK2 alone.

We conclude that GIRK1 and GIRK2 subunits constitute the heteromultimeric inwardly rectifying K^+ channels in the granular layer of the cerebellum. The single point mutation in the highly conserved Gly-Tyr-Gly K^+ channel pore domain of the GIRK2 subunit (*wv*GIRK2) creates a G protein–insensitive, nonselective channel whose basal activity should lead to increased granule cell death in *weaver* mice.

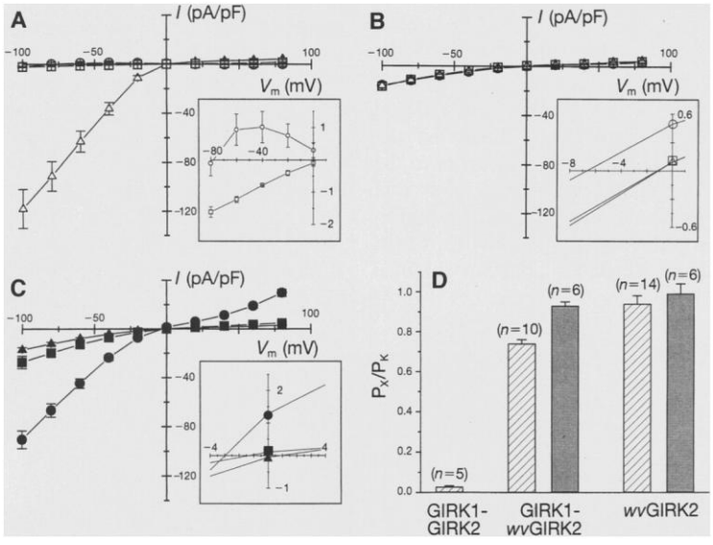

Fig. 2. Lack of selectivity of *wv*GIRK2 channels. Current-voltage relations are shown for CHO cells transfected with cDNAs for (**A**) GIRK1 and GIRK2, (**B**) GIRK1 and *wv*GIRK2, or (**C**) *wv*GIRK2. Recordings were made in the presence of the following external concentrations: 140 mM K^+ (as KCl; triangles), 2 mM K^+ plus 138 mM Cs^+ (squares), or 2 mM K^+ plus 138 mM Na^+ (circles) (140 mM internal K^+ in each case). (**D**) Relative permeability P_X/P_K was determined by measuring reversal potentials when the test ion (X) was on the outside and 140 mM K^+ was on the inside of the membrane. The simplified Goldman-Hodgkin-Katz equation, $V_{rev} = (RT/F)\ \ln\{(P_X[X]_o + P_K[K]_o)/P_K[K]_i\}$ (where R, T, and F represent the gas constant, absolute temperature, and Faraday constant, respectively, and the subscripts o and i represent external and internal concentration, respectively), was used to define the permeability ratio. Data are shown for external concentrations of 2 mM K^+ plus 138 mM Na^+ (striped bars) and 2 mM K^+ plus 138 mM Cs^+ (shaded bars) (140 mM internal K^+ in each case). The reversal potentials were determined at the intersection with the abscissa [insets of (A) to (C)]. Data are shown as means ± SEM.

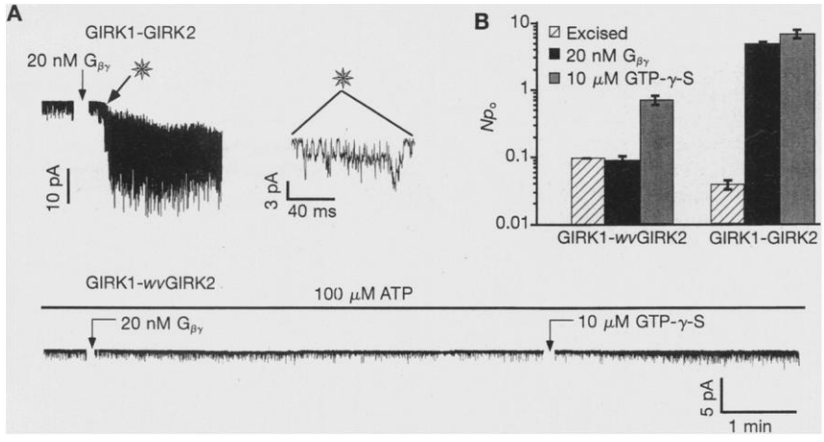

Fig. 3. Insensitivity of *wv*GIRK2-containing channels to $G_{\beta\gamma}$. (**A**) Addition of purified $G_{\beta\gamma}$ subunit dimers to inside-out patches from CHO cells expressing GIRK1-GIRK2 or GIRK1-*wv*GIRK2 (star indicates expanded region). The induced GIRK1-GIRK2 channel activity was high and did not return to baseline during the recording. (**B**) Comparison of average channel activity for $G_{\beta\gamma}$-stimulated GIRK1-*wv*GIRK2 and GIRK1-GIRK2 channels. Each point represents the average of 8 (GIRK1-GIRK2) to 30 (GIRK1-*wv*GIRK2) patches (± SEM); Np_o is plotted on a logarithmic scale.

REFERENCES AND NOTES

1. N. Patil *et al.*, *Nature Genet.* **11**, 126 (1995).
2. G. Krapivinsky *et al.*, *Nature* **374**, 135 (1995).
3. G. Krapivinsky *et al.*, *J. Biol. Chem.* **270**, 28777 (1995).
4. P. Kofuji, N. Davidson, H. A. Lester, *Proc. Natl. Acad. Sci. U.S.A.* **92**, 6542 (1995).
5. B. M. Velimirovic, E. A. Gordon, N. F. Lim, B. Navarro, D. E. Clapham, *FEBS Lett.* **379**, 31 (1996).
6. D. E. Logothetis, Y. Kurachi, J. Galper, E. J. Neer, D. E. Clapham, *Nature* **325**, 321 (1987); K. D. Wickman *et al.*, *ibid.* **368**, 255 (1994); E. Reuveny *et al.*, *ibid.* **370**, 143 (1994); C.-H. Huang, P. A. Slesinger, P. J. Casey, Y. N. Jan, L. Y. Jan, *Neuron* **15**, 1133 (1995); P. A. Slesinger, E. Reuveny, Y. N. Jan, L. Y. Jan, *ibid.*, p. 1145; G. Krapivinsky *et al.*, *J. Biol. Chem.* **270**, 29059 (1995).
7. K. Hedin, N. F. Lim, D. E. Clapham, *Neuron* **16**, 423 (1996).
8. P. Rakic and R. L. Sidman, *J. Comp. Neurol.* **152**, 103 (1973).
9. For in situ hybridization, brains from 6-day-old B6CBA mice were dissected free of the skull and immediately frozen. Sagittal sections were cut, transferred to coated slides, and fixed in paraformaldehyde. Sections were hybridized with digoxigenin-labeled RNA probes with the use of reagents from Boehringer Mannheim according to the manufacturer's protocol. After hybridization at 59°C, sections were washed and incubated with an alkaline phosphatase–labeled antibody to digoxigenin (Boehringer Mannheim) and developed in substrate buffer for 2 to 6 hours in a volume of ~100 μl per slide. Each 100 μl of hybridization buffer contained 100 ng of probe and 50% formamide, 5× standard saline citrate, yeast RNA (1 mg/ml), 1× Denhardt's, 0.1% Tween-20, 0.1% CHAPS detergent, and 5 mM EDTA. Additional information about the expression of GIRK1 and GIRK2 is available at http://peterson02.mc.duke.edu.
10. The 6–amino acid AU5 epitope Thr-Asp-Phe-Tyr-Leu-Lys or the 10–amino acid c-MYC epitope Glu-Gln-Lys-Leu-Ile-Ser-Glu-Glu-Asp-Leu was introduced onto the COOH-terminus of GIRK1 and GIRK2 or *wv*GIRK2, respectively, with the polymerase chain reaction (PCR). One 100-mm dish of COS-M7 cells was transfected with pCDNA3 (Invitrogen) containing the cDNA for the indicated channel subunit or subunit combinations with the use of the *Trans* IT LT-1 reagent (PanVera, Madison, WI). Each dish was labeled for 12 hours with [^{35}S]methionine (50 μCi/ml, Amersham). Cells were lysed in hypoton-

ic buffer, and a crude particulate fraction was prepared. The particulate fraction was centrifuged through a 20% sucrose cushion to remove cytosolic contaminants and then solubilized in 1% CHAPS, 300 mM NaCl, 5 mM EGTA, 5 mM EDTA, and 10 mM Na-Hepes (pH 7.5) buffer supplemented with phenylmethylsulfonyl fluoride (PMSF; 200 μM) and leupeptin, aprotinin, and pepstatin (2 μg/ml each). Immunoprecipitation was done by addition of a 1:200 dilution of centrifuged ascites fluid for either the AU5-specific or the c-MYC–specific (9E10) monoclonal antibodies (BAbCO, Irvine, CA) with GammBind-G Sepharose (5 μl, Pharmacia). Proteins bound to the washed GammBind-G Sepharose were eluted with 1× SDS-sample buffer and analyzed by 10% SDS–polyacrylamide gel electrophoresis followed by fluorography and autoradiography. In immunoprecipitation assays, the AU5-specific antibody did not cross-react with GIRK2, nor did the c-MYC–specific antibody cross-react with GIRK1. Incubation of *wv*GIRK2- or *wv*GIRK2-GIRK1–expressing COS-M7 cells in low-[Na^+] media [*N*-methyl-D-glucamine (NMDG) substituted for NaCl] increased the amount of detectable *wv*GIRK2 and GIRK1 channel subunits in immunoprecipitates. We presume that the lower extracellular [Na^+] increased the number of cells transfected with *wv*GIRK2 or *wv*GIRK2-GIRK1 that survived. NMDG-containing media did not change the expression of wild-type GIRK2 or GIRK1.

11. The Sac II fragment containing the coding sequence of *wv*GIRK2 or GIRK2 was blunt-ended and subcloned into the Eco RV site of the eukaryotic expression plasmid pCDNA1/amp (Invitrogen) under control of the cytomegalovirus promoter. CHO cells were transfected by the calcium phosphate precipitation method (*2, 3*). Each dish was transfected with appropriate combinations of the following: CD4 (a lymphocyte cell surface antigen) in the L3T4 plasmid construct, as a marker for transfection (4 μg) (*4, 5*); pcDNA1/amp (10 μg); pRBG4-GIRK1 (10 μg); GIRK2 (10 μg); or *wv*GIRK2 (10 μg). Transfected cells were identified by anti-CD4 fluorescence and assayed in the tight seal whole-cell patch clamp configuration. The pipette solution contained 140 mM K^+, 142 mM Cl^-, 10 mM Hepes, 5 mM EGTA, 1 mM Mg^{2+}, 1 μM GTP-γ-S, and 0.1 mM ATP (pH 7.3). Bath solution contained 140 mM K^+, 142 mM Cl^-, 10 mM Hepes, 5 mM EGTA, and 1 mM Mg^{2+} (pH 7.3). Whole-cell currents were recorded at 22° ± 2°C with an Axopatch 200A patch clamp amplifier, filtered at 1 kHz (8-pole Bessel filter), and digitized at 5 kHz. Single channels were recorded in symmetrical 140 mM K^+, filtered at 5 kHz (8-pole Bessel filter), and digitized at 25 kHz (pCLAMP6).
12. L. Heginbotham, Z. Lu, T. Abramson, R. MacKinnon, *Biophys. J.* **66**, 1061 (1994); L. Heginbotham, T. Abramson, R. MacKinnon, *Science* **258**, 1152 (1992). P. A. Slesinger *et al.* [*Neuron* **16**, 321 (1996)] have reported a loss of selectivity of truncated *wv*GIRK2 and *wv*GIRK2-containing channels.
13. F. Duprat *et al.*, *Biochem. Biophys. Res. Commun.* **212**, 657 (1995).
14. We thank A. Aleksandrov for helpful discussions and assistance with data analysis, K. Wickman for comments on the manuscript, G. Krapivinsky for purified $G_{\beta\gamma}$, and S. Manahan for assistance with cell culture. Supported by a Colciencias award to B.N., a National Research Service Award award to M.E.K., a Minnesota American Heart Association award to B.V., and an NIH grant to D.E.C. A.S.P. is a Sandoz scholar and is supported by a grant from the National Down Syndrome Society.

23 February 1996; accepted 22 April 1996

A Chemoautotrophically Based Cave Ecosystem

Serban M. Sarbu, Thomas C. Kane, Brian K. Kinkle*

Microbial mats discovered in a ground-water ecosystem in southern Romania contain chemoautotrophic bacteria that fix inorganic carbon, using hydrogen sulfide as an energy source. Analysis of stable carbon and nitrogen isotopes showed that this chemoautotrophic production is the food base for 48 species of cave-adapted terrestrial and aquatic invertebrates, 33 of which are endemic to this ecosystem. This is the only cave ecosystem known to be supported by in situ autotrophic production, and it contains the only terrestrial community known to be chemoautotrophically based.

Nearly all biological communities derive their energy and organic carbon from photosynthesis. In the late 1970s, however, diverse communities were discovered near deep sea hydrothermal vents (*1*). The food base for organisms in this aphotic habitat is supplied by chemoautotrophic organisms that derive their energy from reduced inorganic compounds (*2*). Communities of obligate cave-dwelling organisms often inhabit the aphotic regions of limestone caves (*3*). However, these cave communities rely on organic material transported from the surface as a food base and are thus ultimately dependent on photosynthetic production.

In 1986 access was obtained to a groundwater ecosystem in southern Romania (Fig. 1) having thermal waters of 21°C that are rich in H_2S (*4*). This cave, Movile Cave, contains an abundant and diverse fauna with a terrestrial community composed of 30 obligate cave-dwelling invertebrate species, including 24 endemic species, and an aquatic community of 18 species with 9 endemics (*5*). Air pockets ("airbells") (Fig. 2) in the submerged portion of the cave contain microbial mats composed of fungi and bacteria that float on the water surface and grow on the limestone walls (*6*). Incubation of mat samples with radiolabeled [^{14}C]bicarbonate (HCO_3^-) resulted in the incorporation of radioactive carbon into microbial lipids, indicating chemoautotrophic carbon fixation (*7*). Further, ribulose 1,5-bisphosphate carboxylase–oxygenase, an enzyme characteristic of certain types of autotrophic organisms, is present and active in homogenates made from the mat and in crude cell lysates of bacteria isolated from cave water and cultured in the laboratory (*8*).

In our study we set out to determine whether the chemoautotrophic production observed in the Movile Cave system is also the food base for the invertebrate species inhabiting this ecosystem. We used stable isotope ratio analysis (SIRA) of carbon and nitrogen to determine the relations of selected species to the chemoautotrophic production in the cave. This method is a valuable technique for studying food webs because organisms fractionate isotopes of carbon ($^{13}C/^{12}C$) and nitrogen ($^{15}N/^{14}N$) in predictable ways. Consumers are typically enriched by approximately 1 to 2 per mil in ^{13}C and by 3 to 5 per mil in ^{15}N, relative to their food source (*9*). Samples of microbial mat and of 10 of the 48 species of invertebrates were taken from Movile Cave for isotopic analysis. Some of these cave-limited species

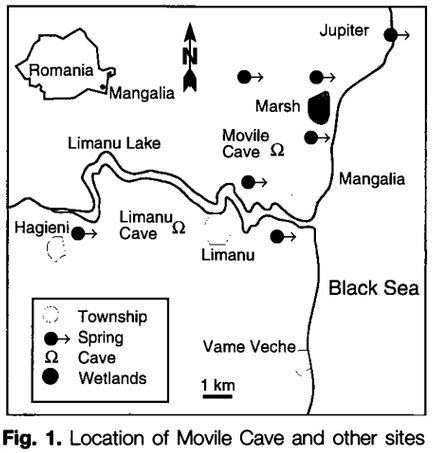

Fig. 1. Location of Movile Cave and other sites from which samples for stable isotope analysis were collected.

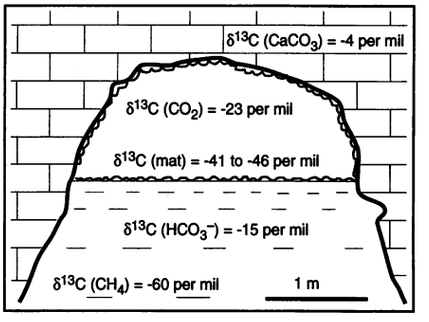

Fig. 2. Cross-sectional view of an airbell in Movile Cave. The atmosphere in the airbells is depleted in O_2 (7 to 10%) and enriched in CO_2 (2.5 to 3.5%) and contains 0.5 to 1.0% CH_4. We determined the atmospheric composition using Draeger tubes.

Department of Biological Sciences, University of Cincinnati, Cincinnati, OH 45221, USA.

*To whom correspondence should be addressed.